APPLICATION OF A GENERAL ANALYSIS FOR SINGLE-SIDED LINEAR INDUCTION MOTORS

C. A. Skalski

Presented at the
CONFERENCE ON LINEAR ELECTRIC MACHINES
London, England
October 21-23, 1974

SUMMARY

The features of a 3-dimensional model for Single-Sided Linear Induction Motors (SLIM) are outlined. This model is based on the discrete (finite) Fourier transform, handles discrete windings, and includes compensation for finite-iron effects. Finite-width reaction rails, with or without side bars, equivalent circuits, and field plots are additional features. The model is compared with experiment and other models, and computer implementation is described briefly.

Introduction

SLIMs are becoming increasingly important for the propulsion of tracked vehicles. To understand the operation of these motors, a computer implemented analysis [1] having the following features was developed:

- Thrust and lift forces, power dissipation in the reaction rail layers, winding impedances, power factor, and efficiency are computed.

- Back iron thickness, conductivity, and permeability are modeled neglecting the effects of iron saturation. Some compensation for effects of saturation is possible by considering an effective permeability, either on a single or multiple layer basis [2].

- Fields are calculated on a three-dimensional basis. The main loss of generality is caused by considering the primary windings and associated iron as represented by a current sheet backed by infinitely permeable iron that has a boundary only at the current sheet. The errors caused by neglecting slots in the iron are correctable using the Carter (or similar air gap) factor. Similarly, errors caused by initially neglecting the finite extent of the primary iron in a real motor are corrected.

- Conventional and unconventional primary windings are easily handled.

- The voltage-drive problem is addressed directly in terms of an equivalent circuit. This circuit is then related to the conventional equivalent circuit for a rotary induction motor.

- Finite width reaction rails with or without sidebars are considered.

- Computer running cost is low, and efficient running on a time-share computer is possible. Field distribution plots can be made quickly and cheaply using the Fast Fourier Transform (FFT) algorithm [3].

The basic mathematical technique used for the analysis is the discrete Fourier transform. Of the various Fourier methods, this approach is most adaptable for computer evaluation. It is similar to use of Fourier series.

A long historical precedent exists for the analytical procedure used. Mention is made of the most important recent references relating to this work. Takahashi et al. [4] and the author's experience in obtaining a general analysis for spherical electromagnetic bearings provided a start. The work of Stickler [5] pointed the way towards a multi-dimensional analysis of SLIMs. Once his own work was well along, the author learned of the work of Oberretl [6]. Of published analyses, Oberretl's is the closest in form to the one outlined here.

Models

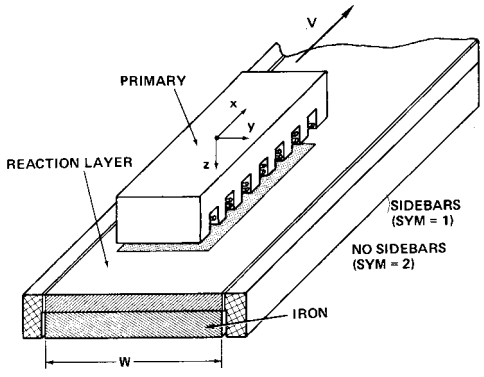

Fig. 1 Slim Models

Figure 1 illustrates the two models considered. The finite length primary is assumed made of highly permeable laminated iron and a plurality of current-carrying coils. The currents in these coils are assumed to have sinusoidal time variation and to be of arbitrary magnitude and phase. The reaction rail consists of a conductor such as aluminum laid over backing iron. Both finite width rails and rails with perfectly conducting side bars can be analyzed. For most practical problems either of the models can be used with comparable results. If the back iron is assumed highly permeable, thick, and non-conducting, the SLIM models may be used to analyze double-sided LIMs on a half-motor basis.

The code SYM=1 is used to designate the model with side bars, while SYM=2 is used for the model without side bars.

Mathematical Procedure

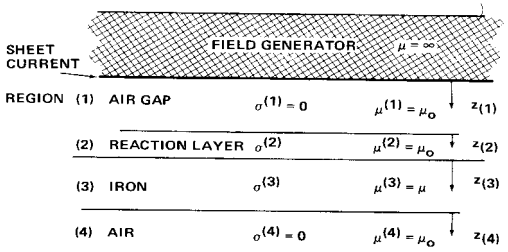

Fig. 2 Layer Structure Considered for Analysis

The layer structure considered for the analysis is shown in Figure 2. The equations used to find the fields in each layer based on layer-fixed coordinates are

$$\nabla^2 A^{(\,)} = \mu^{(\,)}\sigma^{(\,)}\frac{\partial A^{(\,)}}{\partial t} \qquad (1)$$

$$B^{(\,)} = \nabla \times A^{(\,)} \qquad (2)$$

$$E^{(\,)} = -\frac{\partial A^{(\,)}}{\partial t} \qquad (3)$$

A is the magnetic vector potential, μ is permeability, σ is conductivity, **B** is flux density, and **E** is electric field. The appropriate solution to Equation (1) subject to $\nabla \bullet A = 0$ and $A_z = 0$ is

$$A_y^{(\,)} = -\sum_{m,n}\left[B_{mn}^{(\,)}e^{\Gamma_{mn}^{(\,)}z(\,)} + C_{mn}^{(\,)}e^{-\Gamma_{mn}^{(\,)}z(\,)}\right]\bullet e^{jn\alpha y}e^{jm\beta x}e^{j(\omega - m\omega_o)t} \qquad (4)$$

$$A_x^{(\,)} = \sum_{m,n}\left[B_{mn}^{(\,)}e^{\Gamma_{mn}^{(\,)}z(\,)} + C_{mn}^{(\,)}e^{-\Gamma_{mn}^{(\,)}z(\,)}\right]\bullet \frac{n\alpha}{m\beta}\bullet e^{jn\alpha y}e^{jm\beta x}e^{j(\omega - m\omega_o)t} \qquad (5)$$

$$\Gamma_{mn}^{(\,)2} = (m\beta)^2 + (n\alpha)^2 + j\mu^{(\,)}\sigma^{(\,)}(\omega - m\omega_o) \qquad (6)$$

$$\omega_o = \beta V \qquad (7) \qquad\qquad \beta = 2\pi / L \qquad (8)$$

for SYM = 1 $\qquad \alpha = 2\pi / W \qquad (9)$

for SYM = 1 $\qquad \alpha = \pi / W \qquad (10)$

ω is the angular excitation frequency, and ω_o is an angular frequency related to the velocity V. Field quantities in field-generator coordinates are obtained for $\omega_o = 0$. β is related to the Fourier length L. L is usually chosen equal to at least several motor lengths. W, the rail width, is used to define the two values of α, depending on the model chosen.

To find the fields using the above equations, the primary sheet current is first expressed in terms of a Fourier transform, and the boundary value problem is then solved. The divergence of the sheet current **K** is zero and $K_z = 0$. The two remaining components may be expressed by

$$K_x = \sum_{m,n} F_{mn} \bullet \frac{n\alpha}{m\beta} \bullet e^{jn\alpha y} e^{jm\beta x} e^{j\omega t} \tag{11}$$

$$K_y = -\sum_{m,n} F_{mn} e^{jn\alpha y} e^{jm\beta x} e^{j\omega t} \tag{12}$$

where

$$F_{mn} = -\frac{1}{LW'} \int_{-L/2}^{L/2} dx \int_{-W'/2}^{W'/2} dy K_y e^{-jn\alpha y} e^{-jm\beta x} \tag{13}$$

W' = W for SYM = 1 and W' = 2W for SYM = 2. An expression equivalent to Equation (13) may be written in terms of K_x. The F_{mn} are the winding coefficients.

Equations (11) and (12) apply to region (1) with z(l) = 0. At this boundary

$K_y = H_x$ (14) $K_x = -H_y$ (15) where $B = \mu H$ (16)

Continuity of B_{normal} and $H_{tangential}$ is required at the remaining boundaries defined by z( ) = 0, and all fields must vanish for z(4) infinite. Solution of the boundary value problem results in 7 complex linear equations that must be solved simultaneously.

These equations are put in tri-diagonal form and then solved for the $B_{mn}^{(\,)}$ and $C_{mn}^{(\,)}$ using an algorithm specially suited to this situation [7].

All solutions of Equation (13) considered here are for K_y given by the super-position of terms corresponding to individual conductors. These have the form

for y corresponding to the primary $K_y' = I_0 e^{j\phi} \delta(x - x')$ iron.

Io is current magnitude, ϕ is the phase of the current, and x' is the conductor location. δ is the impulse (Dirac delta) function. For SYM = 1, all conductors are considered symmetrically positioned with respect to the line y = 0. For SYM = 2, conductor pairs (i.e., motor pairs) are considered such that a conductor lies to

either side of the axis y = 0 and the currents are of opposite phase. This condition causes transverse current flow to be zero at y = 0, ±W. Cuts (rail edges) can then be considered to exist there. Similar logic applies to introduction of perfectly conducting side bars for the SYM = 1 model at lines where only transverse current flows, y = ±W/2.

Using the magnetic field B(2), it is a simple matter to find the forces by surface integrations of the Maxwell stress tensor at z(2) = 0. The power losses in the reaction layers are readily found using E(2) and E(3). Also, the winding impedances are found using E(1) at z(1) = 0. Rather than deal with the phase impedances individually, it is convenient to deal with the average phase impedance Z = R + jX.

Equivalent Circuits

The left equivalent circuit in Figure 3 is used to solve the voltage-drive problem once a solution has been obtained with current drive. Added to the average phase impedance Z are the winding resistance R1 and the additional leakage reactance X1L. The lower equivalent circuit applies primarily to rotary induction motors. It is of considerable importance to LIM practice because of wide use by manufacturers. The values of R1, the leakage reactance X1, and the magnetizing reactance XM can be assumed to be reasonably correct as specified by a manufacturer. Using these values and the topmost circuit, it is easy to determine the values of the secondary resistance R2 and leakage reactance X2 that make the two circuits equivalent. R2 and X2 are both strong functions of slip in LIMs exhibiting significant end effect. A comparison of computed and manufacturer-specified R2 and X2 can provide useful insights into motor behavior and can help in communicating with designers employing traditional methods.

The X1L used here is a fraction of X1, since it is a part of X1. The range on this fraction is .5 - .8 for three motors that have been subjected to preliminary analysis using the theory presented here. In all cases, X1L was determined so as to obtain a correspondence between computed and measured voltage and current at one operating point. Once X1L is found for a particular motor, its value should not be altered during analysis.

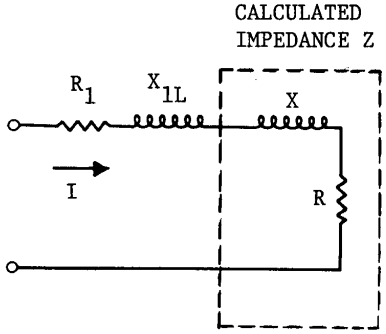

Figure 3A Mitre Model

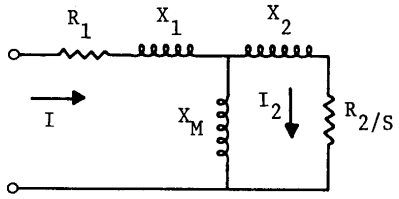

Figure 3B Conventional Rotary Induction Motor Model

Use of the Analysis

Numerous computations have been made for the LIMRV [8] and TLRV [9] double-sided LIMs. These are preliminary in nature and have served to refine the theory. Comparisons have been made with experimental data, with computations made by Elliott using his mesh/matrix method [10], and with predictions made by the manufacturer of the LIMRV and TLRV motors. The comparison with predictions by Elliott is considered especially important because he specifically addresses the problem of finite iron and his analytical procedure is radically different from the one presented here. Mosebach [11] has considered the finite iron problem by a conformal mapping and the use of Fourier methods. His findings along with Elliott's provide valuable insight into the magnetic wake problem.

The equations for fields, forces, and powers involve summation over the indices m and n. An additional level of summation is needed for the winding coefficients (over the number of coils) and for refined computation of lift force. The ranges on m and n are chosen symmetrically about zero, preferably as powers of 2 for FFT compatibility. The range on m, which is associated with the longitudinal direction x, is +(IB - 1). An IB = 32 has proven very adequate for the 10 pole LIMRV motor when the Fourier length L is 5 motor lengths. For high speeds and low slip, check computations have been carried out with IB = 64 and L = 10 motor lengths. The adequacy of L has also been checked by making plots of the normal flux density distribution at the surface of the reaction layer. The 5 pole TLRV motor has more of an end effect than the LIMRV motor. Its needs in terms of IB and L are slightly more demanding. No harm is done in making IB and L as large as possible except to waste computer time and introduce the possibility of numerical errors.

The Fourier width is defined by reaction rail width. The range on the index n is ±(IC - 1). As IC is varied from a small value towards a large value, rapid convergence is observed on the thrust computation for a constant-current drive

but not for a constant-voltage drive. This appears as a rapid convergence on the value of R and a slow convergence on X in the equivalent circuit. The secondary reactance X is thus mildly dependent on the value of IC. A practical LIM, however, cannot be described by infinite IC because of finite primary iron. The effective sheet current for a practical motor exhibits a finite slope at the side boundaries of the primary iron. Estimates for IC have been derived on the basis of matching this slope for Ky to the slope of B_z estimated using a magneto-static analysis [12].

This analysis gives the slope for magnetic field normalized to its peak value as $|dB_{norm}/dy| = 1/(4G)$, where G is the magnetic air gap and the slope is given at $B_{norm} = 1/2$. The validity of the slope estimate has been checked against experimental data presented by Preston and Reese [13], and Bolton [14]. Agreement exists to within 50%, which is considered good enough. The estimates obtained for IC by slope matching are

$$IC \approx W/(8G) + 1 \qquad \text{for SYM = 1 and}$$

$$IC \approx W/(4G) + 1 \qquad \text{for SYM = 2}$$

The values of IC used for analysis of the LIMRV and TLRV motors are 4 for SYM = 1 and 8 for SYM = 2. Making IC a power of 2 is important for FFT compatibility.

While infinite primary iron in the transverse direction creates difficulties in obtaining an accurate voltage-drive analysis, infinite iron in the longitudinal direction produces a false magnetic wake. The false wake is substantially longer than the real wake for high velocity and low slip. In terms of magnetic field inside the motor, the false wake does not have much effect on its value. Thus, force computations based on the field inside the motor could be expected to yield accurate results. Integration of the stress tensor over the entire Fourier expansion area is normally used and results in a twofold summation. Stopping the integration to cut off the false wake produces a threefold summation. This results in extra computation time, which is sometimes justified for more accurate lift computations. It is not necessary for accurate thrust computations, since the false wake has little effect on thrust. The making of lift computations with truncation of the wake is an option in the computer program. When used, lift is computed both with and without the wake, so that a comparison can be made. The boundaries usually chosen for truncation are one air gap away from the leading and trailing edges of the primary iron.

Reluctance (iron edge) end forces occur in a practical finite-iron LIM. Dukowicz [15] has found these forces to be small. Skalski [12], using a different procedure, has estimated these forces in the high-speed limit for electromagnets.

Electromagnet drag when strong end effect is present and the magnet is made of highly permeable unsaturated iron may be estimated using

$$F_{drag} \approx B_0^2 W' G / (2\mu_0) \qquad (17)$$

Equation (17) may be applied to LIMs by taking B_0 = flux density at rear edge of primary, W' = width of primary iron, and G = magnetic air gap. The result obtained using Equation (17) should be subtracted from the thrust computed with infinite iron. Except for very small slip values, this correction will be small. Equation (17) is not easily applied, since B_0 must be known. Most practical computations are not expected to require correction for reluctance force.

Some Results

The analysis presented here has been used to make numerous predictions for the LIMRV motor. Comparisons with experimental data obtained to speeds of 292 km/hr reveal reasonably good predictions of thrust, current, efficiency, and power factor. Additionally, agreement with the manufacturer's predictions is reasonable.

Elliott using his mesh/matrix method has made predictions for the LIMRV motor. Comparisons with his thrust predictions for operation at 403 km/hr indicate good agreement. Also, his predictions for lift force (LIMRV operation as a SLIM) proved very helpful in the study of the false wake occurring with infinite iron models. For slip in the range .05 to .13, the false wake was observed to produce a lift comparable in magnitude to that produced by the fields inside the primary. Truncation of the false wake produced lift predictions in accord with those of Elliott.

Numerical and analytical accuracy has been checked by testing for energy conservation. The ratio of electrical input power to the total output power is computed at each operating point. This ratio is printed as 1.00000 if no error is indicated to the number of places shown. A perfect result has been obtained for all motor problems solved to date with a computer using a 14 digit mantissa. Errors in the fourth and fifth places have been observed on occasion when solving electromagnet problems.

Field distribution plots made for the LIMRV motor show L = 5 motor lengths is adequate for slip greater than .05 and speeds to 403 km/hr. Transverse plots show field dips in the center of the primary of the type discussed by Preston and

Reese [13], and Bolton [14]. The shape of longitudinal field distributions has been found to be significantly dependent on the transverse position (y).

Conclusions

The discrete (finite) Fourier transform permits fast 3-dimensional solutions of SLIM problems. Although basic problem formulation is based on an infinite primary iron model, corrections are introduced to account for finite iron effects.

Preliminary use of the analysis as implemented on a time-share computer system reveals it is easy to use, low in operating cost, and capable of yielding accurate results. The state of development of the theory is considered adequate for immediate purposes. Special problems are bound to become apparent as more experimental data is processed, new modes of operation considered, etc. The theory has the flexibility needed for adaptation to many new situations. In some instances, however, methods such as Elliott's mesh/matrix, numerical analysis using finite differences, etc. will be necessary in spite of their substantially greater computing cost.

ACKNOWLEDGMENT

In addition to individuals mentioned in the paper, special thanks are due Mr. J. Duncan of the Ontario (Canada) Ministry of Transportation and Communications for many helpful discussions, and the U.S. Federal Railroad Administration for furnishing useful advice and providing sponsorship of the work on the LIMRV and TLRV motors.

REFERENCES

1. C. A. Skalski, "A General Analysis for Linear Induction Motors and Electromagnets," MITRE Technical Report, in preparation); July 1974.

2. M. F. Alves and P. E. Burke, "Single-Sided Linear Induction Motor with Magnetic Material in the Secondary," IEEE Conference Record of IAS/1973, Eighth Annual Meeting, Milwaukee, Wisconsin, U.S.A., pp. 321-329 ; 8-11 October 1973.

3. G. D. Bergland, "A Guided Tour of the Fast Fourier Transform," IEEE Spectrum, pp. 41-52; July 1969.

4. N. Takahashi, S. Kawai, and K. Akihashi, "Analysis of Rail Eddy-Current Brake for High-Speed Railroad Vehicles," Electrical Engineering in Japan, v. 90, n. 2, pp. 95-104; 1970.

5. J. J. Stickler, "Study of Reaction Forces in a Single Sided Linear Induction Motor (SLIM)," Report FRA/ORD&D-74-28 (May be ordered from NTIS, Springfield, Va. 22151, U.S.A.); January 1974.

6. K. Oberretl, "Dreidimensionale Berechnung des Linearmotors mit Berucksichtigung der Endeffekte und der Wicklungsverteilung," Simposio Sur Motori Lineari, Capri; 19-21 June 1973.

7. B Carnahan, H. A. Luther, and J. O. Wilkes, Applied Numerical Methods, Wiley, New York and London, pp. 441-442; 1969.

8. Garrett Corporation (AiResearch), Linear Induction Motor Research: Linear Induction Motor and Test Vehicle Design and Fabrication, NTIS No. PB221608 (See Ref. 5); October 1971.

9. Garrett Corporation (AiResearch), Development and Manufacture of a Linear Induction Motor Propulsion System for the Tracked Air Cushion Research Vehicle, NTIS No. PB 2129777 (See Ref. 5); April 1971.

10. D. G. Elliott, "Numerical Analysis Method for Linear Induction Machines," 12th Symposium on the Engineering Aspects of Magnethohydrodynamics, Argonne National Lab., Argonne, Ill.; 27-29 March 1972.

11. H. H. Mosebach, Technishe Universitat Braunschweig, Germany, Lecture and Discussion at U.S. Department of Transportation, Washington, DC, 18 April 1974.

12. C. A. Skalski, "Characteristics of Electromagnets for Levitation of Tracked Vehicles," MITRE Corp. Report; 1974.

13. T. W. Preston and A. B. J. Reece, "Transverse Edge Effects in Linear Induction Motors," PROC. IEE, v. 116, n. 6, pp. 973-979; June 1969.

14. H. Bolton, "Transverse Edge Effect in Sheet-Rotor Induction Motors," PROC. IEE, v. 116, n. 5, pp. 725-731; May 1969.

15. J. Dukowicz, "Analysis of Linear Induction Machines with Discrete Windings and Finite Iron Length," IEEE Conference Record of IAS/1973 Eighth Annual Meeting; Milwaukee, Wisconsin, U.S.A., pp; 311-319; 8-11; October 1973.